International Journal on Science and Technology (IJSAT)

E-ISSN: 2229-7677 ● Website: www.ijsat.org ● Email: editor@ijsat.org

From Simulations to Clinical Practice: The Impact of 4D XCAT Phantoms on Imaging Technologies

Fadwa Joma Abuhbail

Faculty of medical technology,misrata libya
Email:nanan4428@gmail.com

Abstract

The purpose of the four-dimensional (4D) eXtended CArdiac-Torso (XCAT) phantom series was to create precise computer models of human anatomy and physiology. The XCAT series includes parameterised models for the respiratory and cardiac movements and includes a large population of phantoms ranging in age from birth to adult. Numerous body sizes, various anatomies, cardiac or respiratory motions or patterns, patient positions and orientations, and spatial resolutions can all be mimicked with the XCAT thanks to its very flexible design. Because of this, XCAT phantoms are becoming increasingly used in biomedical imaging research.They can offer a virtual patient base from which imaging instrumentation, data acquisition, methodologies, and image reconstruction and processing methods can be statistically evaluated and improved. This can result in better picture quality and more precise clinical diagnoses. Radiation dosimetry, radiation therapy, medical device design, and even the security and defence sector have found extensive applications for the phantoms. This review study focusses on a few specific applications of the XCAT phantoms in biomedical imaging and related sectors. We demonstrate the growing significance of computer simulation and computerised phantoms in the scientific community with these instances.

Index Terms—Biomedical imaging phantoms, CT, dosimetry, image analysis, image reconstruction, medical diagnostic imaging, medical simulation, PET, and SPECT

1. INTRODUCTION

Computer simulation is a vital tool in many contemporary scientific and technical fields for testing and fine-tuning novel technology. By means of simulation, scholars Copyright (c) 2017 IEEE. Personal use of this material is permitted. However, permission to use this material for any other purposes must be obtained from the IEEE by sending a request to pubs-permissions@ieee.org. Paper was submitted February 14, 2017. This work was supported by the research grant R01 EB001838 from the National Institutes of Health. W. Paul Segars is with the Carl E. Ravin Advanced Imaging Laboratories, Department of Radiology, Duke University Medical Center, Durham, North Carolina 27705 USA. (e-mail: paul.segars@duke.edu). B.M.W. Tsui is with the Division of Medical Imaging Physics, Department of Radiology and Radiological Science, the Johns Hopkins University, Baltimore, Maryland

21287 USA. Jing Cai and Fang-Fang Yin are with Department of Radiation Oncology, Duke University Medical Center, Durham, North Carolina, 27705 USA.

is an Adjunct Assistant Professor, Department of Radiology in Johns Hopkins Radiology and Radiological Science, the Johns Hopkins University, Baltimore, Maryland 21287 USA. He is also an employee of Siemens Medical Solutions USA.

Ehsan Samei is with the Carl E. Ravin Advanced Imaging Laboratories, Department of Radiology, Duke University Medical Center, Durham, North Carolina 27705 USA.
are capable of carrying out experiments solely using a computer.
In order to conduct certain studies, precise computer algorithms based on physics are employed to operate on or interact with computer-based human body models, or phantoms. The researcher has total control over the subject's anatomy and the experimental conditions, enabling them to conduct whatever kind of study they choose. Because of this benefit, simulation is now a crucial addition to theoretical inferences, experimental procedures, and research in the fields of biomedical imaging and other development.The use of computerised phantoms in simulation is significant. Because of this, a wide variety of models have been created over time. A total of four hundred phantoms have been created by various universities and companies to study dosimetry and medical imaging applications, as indicated in Tables 1-3 and Fig. 25 of the George Xu1 article.Numerous further phantoms have been created for applications in the disciplines of bioengineering, medical device design, and other fields2–7.These sources cover a very minor portion of the state of the art. This special issue features a wide variety of phantoms.As part of our study, we created the 4D XCAT phantom8, a computational model of human anatomy and physiology intended mainly for use in imaging-related biomedical applications. The evolution of the XCAT over time is depicted in Figure 1. Originally, the XCAT phantom was a male torso model.
The 4D NURBS-based cardiac-torso (NCAT) phantom9–11 was the name given to this initial iteration XCAT system. The purpose of its development was to examine the impact of motion on nuclear medicine imaging, particularly PET and SPECT (single-photon emission computed tomography). The NCAT's organs and structures were defined by hand.

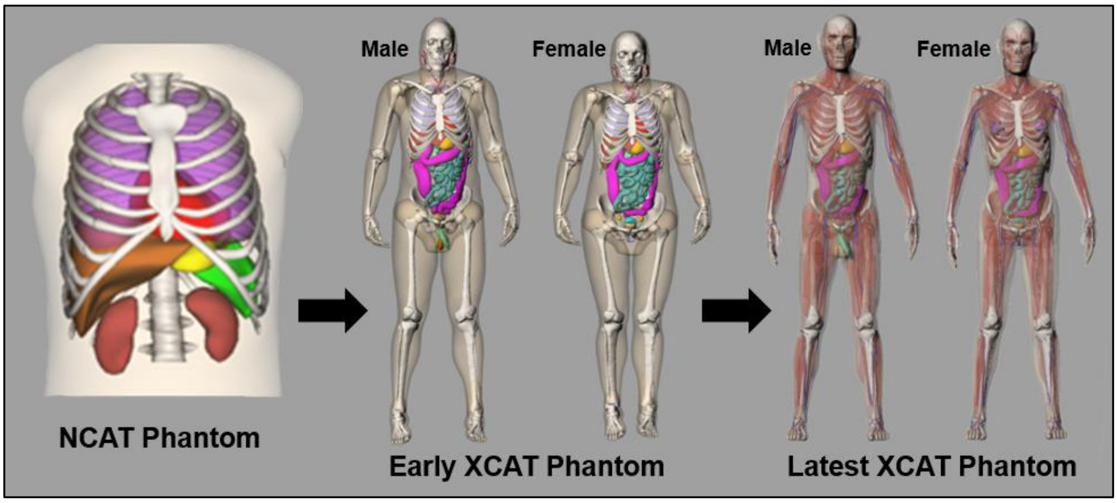

Figure 1. The NCAT, a model of the male human torso, served as the ancestor of the XCAT phantom.

Females were represented by adding breast surfaces to the torso. The most recent XCAT phantom models were created by expanding the NCAT by incorporating more intricate features and separating male and female anatomy.

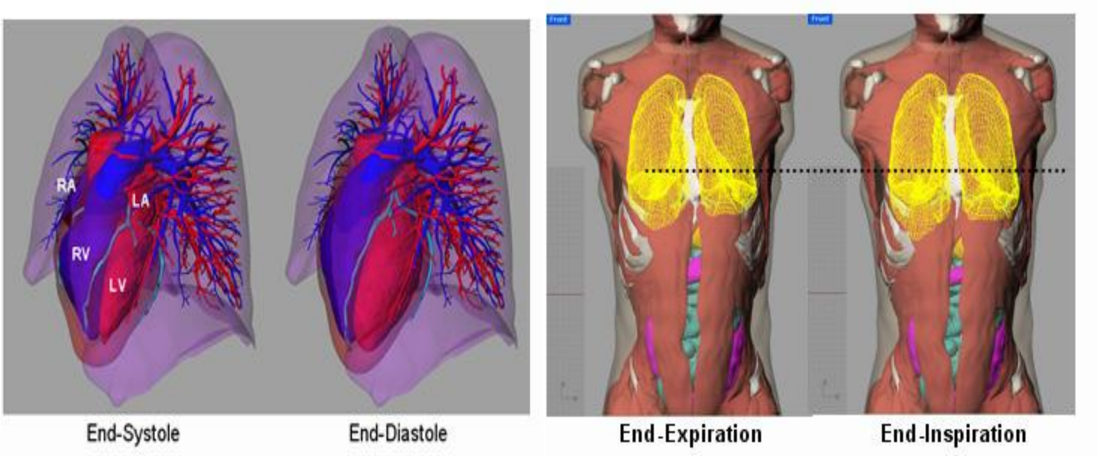

Fig. 2. Cardiac and respiratory models of the XCAT phantom. Each includes a set of parameters to simulate different normal and abnormal motions.

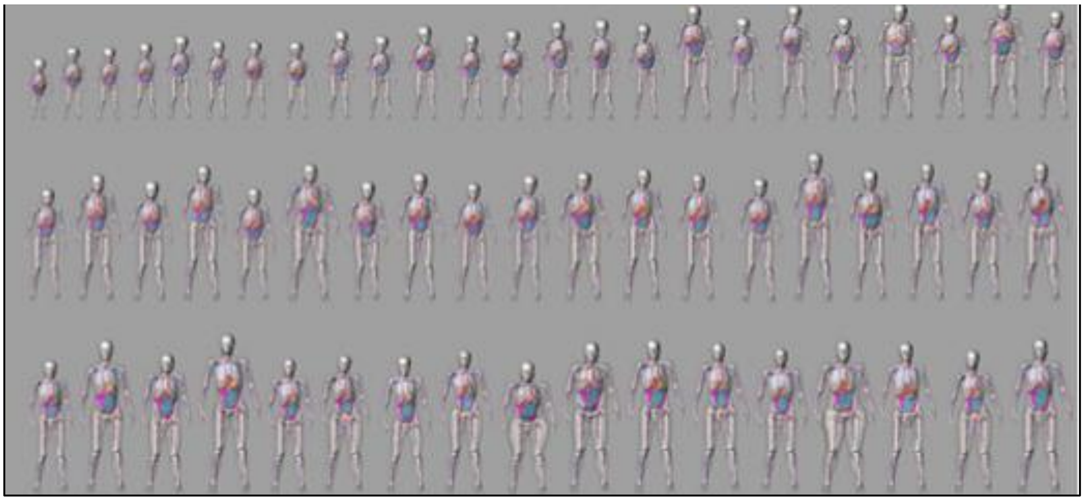

Fig. 3. Population of new XCAT models. Selected models at various ages, heights, and weights are shown.

Utilising the SURFdriver program (www.surfdriver.com) to segment the Visible Human Male x-ray computed tomography (CT) dataset from the National Library of Medicine (NLM). Then, using SURFdriver, 3D polygon models were fitted to each segmented structure and loaded into www.rhino3d.com, a rhinoceros modelling program. Each of the polygon models had thousands of triangles in it. Using Rhinoceros, cubic non-uniform rational b-spline (NURBS) surfaces were fitted to each polygon model for a more condensed definition.Hybrid phantoms, a new class of computational models, were first developed by the NCAT phantom1. At first, these phantoms are described as collections of divided patient imaging data. The structures are then defined using surface representations like NURBS. The additional flexibility to alter the structures to represent patient motions or anatomical differences is provided by the surface definition, which can be applied to the points that define the structures' shape. Based on deformations obtained from 4D cardiac and respiratory CT data, the NCAT phantom was configured with models for the beating heart and breathing motions9.

By further segmenting the Visible Human Male and Female whole body CT datasets, the NCAT was first expanded into whole-body male and female models, resulting in the first iteration of the XCAT phantom. The XCAT phantom was then redesigned using the Visible Human anatomical datasets from the NLM8 to offer an even greater degree of anatomical information.The individual body slices were captured in colour, much higher resolution images (0.33 mm pixel size against 0.898 mm for the CT scan) that made up the anatomical data. on a tablet computer, the anatomical images were segmented using a graphical program called Image Segment that was created in our lab. Because Image-segment let users to omit slices when contouring an object, it made segmentation more efficient than SURFdriver; The interpolation between the slices was done using cubic spline interpolation. Using Image Segment, the segmented structures were transformed into polygon models, which Rhinoceros then fitted with NURBS surfaces. The anatomies of men and women were modelled using thousands of surfaces. Every muscle, blood artery, and bone have their own surfaces.In terms of bodily habitus, the male and female subjects of Visible Human were both larger persons. The PeopleSize anthropometric software, www.openerg.com/psz/index.html, and the International Commission on Radiological Protection (ICRP) Publication were used to match 50th percentile characteristics in terms of body size and organ masses for the XCAT male and female models, using the flexibility of the NURBS.Figure 3 illustrates how the XCAT male and female models were expanded into a population of models that represent the human body at different ages, heights, and weights from newborn to adult13–15 using techniques from computational anatomy. Using segmented patient CT data as a guide, a template XCAT anatomy (male or female) is altered (by applying a high-level transformation to the surface points) to match the anatomical framework. The technique enables the creation of new, highly detailed phantoms with efficiency since it eliminates the need to segment every structure from the CT data.Certain muscles, blood arteries, and other structures that are difficult to segment can be filled in with the modified template. Every new model includes the same level of cardiac and respiratory models and anatomical definition as the original template.The first four-dimensional library of computational models combining temporal and spatial information is made up of the XCAT series of phantoms. They offer representative samples of the variance in a population and realistically simulate the human anatomy, heart, and breathing motions. Because of their surface definition, they also possess a significant deal of flexibility. The phantoms do not yet statistically characterise the anatomy, in contrast to 3D shape models16 that are utilised for atlas-based segmentation and comparisons of forms or physiological parameters within a population. All phantoms, however, can be used as a springboard to build new models by applying user-specified deformations. It is possible to build an infinite variety of anatomies, motions or patterns, subject location, and orientation.Scientific study is increasingly utilising the 4D XCAT due to its exceptional versatility and high level of realism. The phantoms are accessible to numerous research labs within for-profit imaging corporations (such as GE, Philips, Siemens, Samsung, and Microsoft) and hundreds of imaging-focused academic institutions worldwide. The phantoms have also been obtained by the radiation dosimetry, radiation oncology, and defence industries for their respective fields of use.
The NCAT/XCAT phantoms have been used in more than 150 peer-reviewed academic articles (excluding the authors of this paper), according to PubMed. The various uses for these papers are listed

in Table 1. Each application's total number of papers discovered is provided, along with five carefully chosen references.

Table 1. Application of the NCAT/XCAT phantoms by other researchers according to peer-reviewed publications listed in PubMed.

Application (with selected references)	**Total number of papers**
CT imaging methods (image quality, image processing, and quantitation)17-21	11
CT image reconstruction22-26	12
SPECT/PET imaging methods (image quality, image processing, and quantitation)27-31	31
SPECT/PET image reconstruction32-36	24
PET/SPECT attenuation, scatter correction37-40	17
SPECT collimator/detector optimization41-45	6
MRI imaging methods (evaluation and image processing)46-50	5
Radiation Dosimetry51-55	12
Radiotherapy56-60	11
Motion (effect, estimation, and compensation)61-65	23

We highlight particular applications of the XCAT phantoms (in its many forms) in this review paper. These fields encompass other bioengineering applications in addition to some of the previously mentioned subjects. We demonstrate how computer simulation and computerised phantoms can be essential research tools through the instances that are given.

2. EVALUATION OF MEDICAL IMAGING TECHNIQUES

The XCAT phantoms were first intended to be used as virtual patients in biomedical imaging research in order to assess and enhance imaging methods and apparatus. Clinical trials would be the perfect means of achieving this kind of review. However, trying to conduct a clinical trial for the numerous novel intricacies of an expanding array of technological products is incredibly expensive and unfeasible. A number of configurable factors are involved in the capture, reconstruction, processing, and interpretation of images in each imaging technique. Testing every potential combination of parameters and task on every possible patient type under clinical conditions is practically and ethically impossible.In clinical assessments, physical phantoms66 might be employed as a patient stand-in. They could have genuine anatomical forms or just be basic test devices. Even 3D printing of them from computer models is possible67. Physical phantoms do have one drawback, though: making a number of models that accurately depict a range of patient sizes and variations would be quite costly, especially when motion is taken into account.An technique to optimisation and evaluation that is more useful is provided by computer simulation. A virtual patient in imaging simulation is represented by a computerised phantom, such as the XCAT. After that, it is photographed using a precise computerised

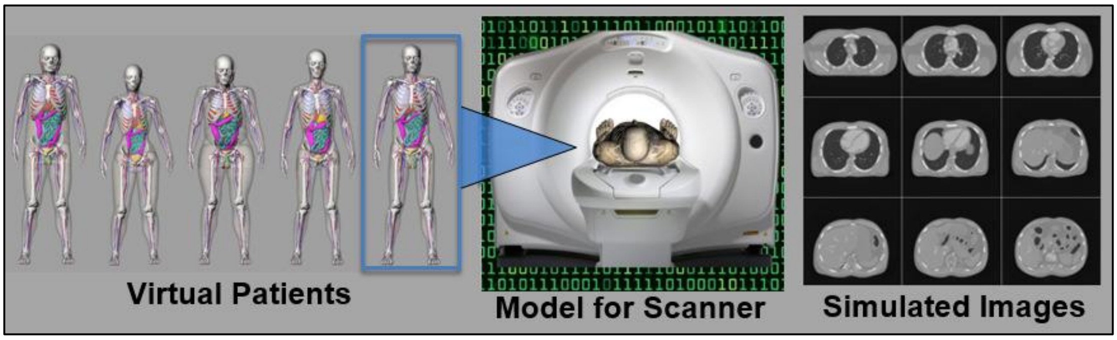

Fig. 4. Computed tomography (CT) simulation using an XCAT phantom chosen from the population.

model of the imaging system, including the physics of the imaging process and its performance characteristics. Recent developments have allowed for the precise modelling of a variety of imaging systems through the use of Monte Carlo (MC) and analytical techniques. Patient-quality imaging data from several modalities can be produced by combining computerised phantoms with imaging process models, as shown in Fig 4.Clinical trials can be carried out remotely thanks to these simulation tools, which give the user total control over the imaging apparatus, procedure, and patient anatomy. Because the phantom's precise anatomy is known, there is a "gold standard" or "truth" that can be used to quantitatively assess how the imaging system, technique, acquisition procedure, image reconstruction, and processing processes affect the quality of the final image. The imaging system and imaging method might have an adverse effect on the quality of the images. One may see how different approaches and related parameters affect the final photos as compared to the known phantom by adjusting the system design settings.The imaging technique parameters and system architecture that yield the best image quality for a particular task can be chosen. To evaluate the risk of radiation exposure to patients, the radiation dosage to the organs and anatomical structures from various protocols can also be computed. Using live subjects is not possible for any of these.Because of the benefits that simulation provides, 4D

XCAT has been widely used in biomedical imaging research to examine how anatomical, physiological, physical, and instrumentational factors affect imaging outcomes. It has also been used to examine image acquisition strategies, processing and reconstruction techniques, and visualisation methods, all aimed at enhancing image quality for more precise diagnosis. We've highlighted a few of the XCAT's uses in these fields below. Please take note that the NCAT phantom is mentioned in the references for a few studies. The NCAT is the first generation XCAT phantom, as was previously described.

A. Comparison of Reconstruction Methods: Gated Myocardial Perfusion SPECT

The XCAT phantom and its model for cardiac motion were utilised in a series of investigations by Lee et al. 68–71 to assess various reconstruction techniques in myocardial (MP) SPECT. A male adult (50th percentile for height and weight) with normal cardiac motion and aberrant motions, such as anomalies related to perfusion and wall motion, was simulated using the XCAT. An analytical projector model was employed to replicate the process of SPECT imaging. Data on projections incorporating the effects of attenuation, dispersion, and collimator-detector response were produced, with 8 and 16 gates/cardiac cycle.

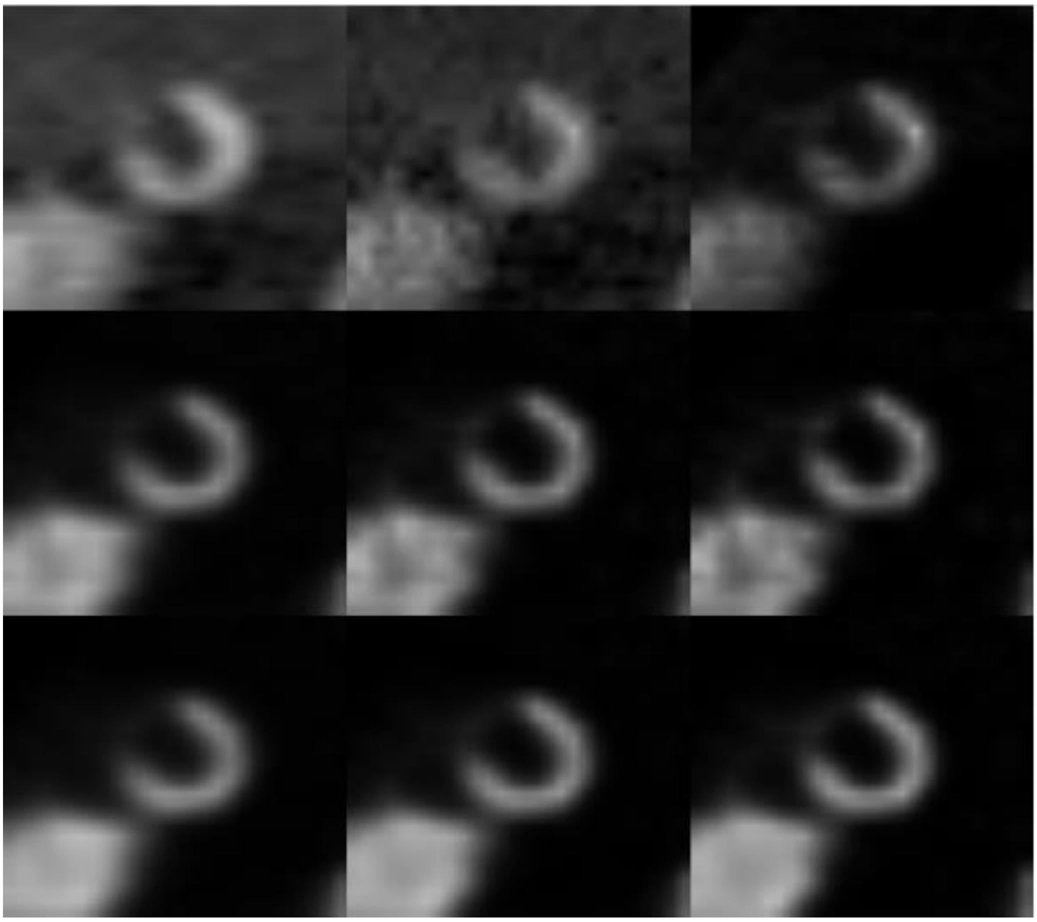

Fig. 5. The first frame of the short axis reconstructed images of the XCAT heart in an 8 frame cardiac gating scheme (Top left to right: FBP (ramp, cutoff=0.25), FBP (ramp, cutoff=0.5), and OS-EM without any correction (16 updates); Middle: OS-EM with ADS corrections (16, 32, 48 updates); Bottom: 4D RBI-MAP with ADS corrections (16, 32, 48 updates)

(ADS). The final visuals may be deteriorated by these instrumental and physical influences. Several techniques were used to reconstruct the projection data: 3D ordered subset expectation maximization (OS-EM) with ADS corrections, 3D filtered back projection (FBP) without ADS corrections, and a proposed 4D rescaled block iterative maximum a posteriori (RBI-MAP) algorithm that incorporates both an ADS correction and a correction for cardiac motion.

The outcomes of the various techniques for eight gates that were reconstructed throughout the cardiac cycle are displayed in Figure 5. It is evident that improving the reconstructed images involves accounting for the physical effects of attenuation, detector response, and scatter. The best results are obtained by further correcting motion using the 4D RBI-MAP approach, as confirmed by human observer studies71 and image quality indicators (normalized mean squared error and averaged normalized standard deviation).As new approaches to image collection and reconstruction have been developed, computer phantoms and simulation tools offer a practical way to test and improve these methods. As indicated in Table 1, the XCAT has been utilized to examine numerous reconstruction methods in PET, SPECT, and CT.

B. Effect of Anatomy

Assessment of Quantitative Imaging Techniques for Estimating Residence Time and Organ Activity The XCAT phantom can be used to study how anatomy affects medical imaging methods because it can be used to simulate various body types. In order to assess quantitative imaging techniques in radioimmunotherapy, He et al.73 created an initial population of 49 phantoms with realistic variances in patient anatomy, biodistribution, and biokinetics.111Monte Carlo simulation methods were used to model SPECT and planar data from the phantom population in ibritumomab tiuxetan. The accuracy and variation in accuracy of residence time estimation techniques that employed a time series of SPECT and planar scans were assessed using the phantom projections.The findings showed that the processing techniques varied in terms of their average accuracy as well as how the accuracy varied among the phantom population. The phantom fluctuations caused more accuracy variations than the noise (less than 2%, according to a prior study). This highlights how crucial it is to use phantom populations in order to objectively assess imaging techniques by capturing the effects of various anatomies.

C. Effect of Respiratory Motion: CT-based Attenuation Correction in SPECT

Patient voluntary, respiratory, and cardiac motions can all produce distortions in medical pictures that could result in a patient being misdiagnosed. To investigate these impacts and create compensatory techniques, the XCAT phantom can be used to simulate various motions. A sample study72 employed the phantom to test the impact of CT-based attenuation correction (CTAC) on reconstructed SPECT pictures and assess the degree of respiratory artifacts using various CT scanners, ranging from single-slice to cutting-edge multi-slice devices. In order to generate In-111 ProstaScint and Tc-99m Sestamibi SPECT emission projection data, various patient breathing patterns were realistically modeled using the XCAT phantom.The effects of respiratory motion were examined in both the CT and reconstructed SPECT pictures.

Example simulated and acquired respiratory artifacts in a delayed acquisition CT scanner are displayed in Figure 6. It was discovered that these artifacts impacted CTAC SPECT reconstructions and increased with decreasing rotation speeds. The fastest CT scanner was shown to produce artifacts in the SPECT

International Journal on Science and Technology (IJSAT)
E-ISSN: 2229-7677 ● Website: www.ijsat.org ● Email: editor@ijsat.org

reconstructed images because of the discrepancy between the CT (breathhold) and SPECT (average motion) data, even though it was less sensitive to motion.

D. Effect of Cardiac Motion on CT and MRI

A useful simulation has been offered by the XCAT phantom.

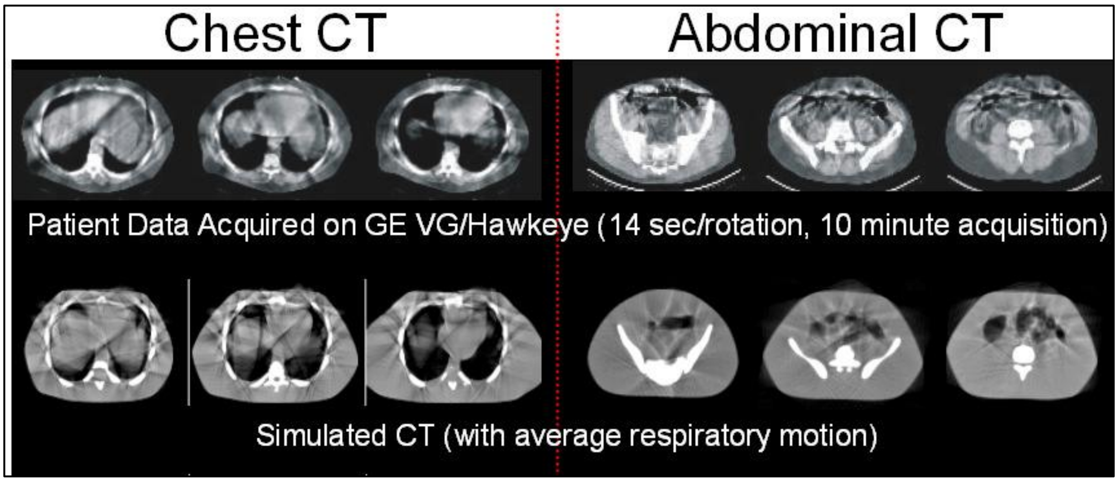

Fig. 6. (Top) Type of respiratory motion artifacts that can occur in CT images acquired with a slower acquisition scanner (14 seconds per rotation) . Artifacts appear as streaks and discontinuities. (Bottom) Simulated images generated from the 4D XCAT show similar artifacts.

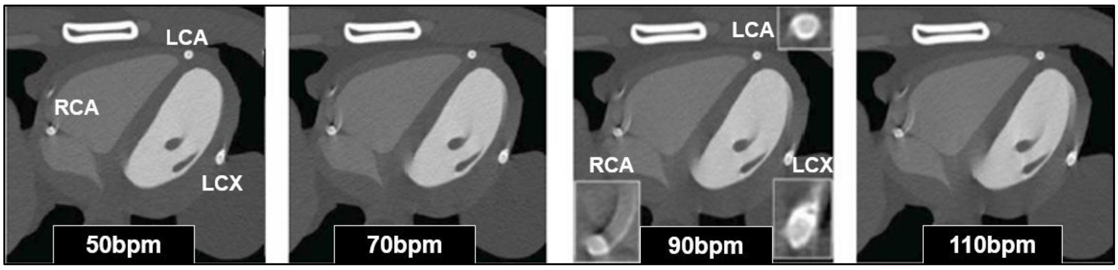

Fig. 7. Coronary CT angiography simulation using the 4D XCAT phantom with coronary stents and the heart beating at (left to right) 50bpm, 70bpm, 90 bpm and 110bpm74. Artifacts from the cardiac motion can be seen as streaks around the coronary vessels (zoom-ins shown for 90 bpm)

Instrument to investigate the impact of heart motion as well. As an illustration of this study, Fung et al.74 examined the impact of varying stent diameters and heart rates on CT angiography pictures using the XCAT cardiac model.

Patients with and without cardiac motion at varying heart rates (50–110 beats per minute) were simulated using the 4D XCAT. The coronary arteries were filled with a variety of stents that were known to be the right size and position. Each case's CT data was produced using Siemens Healthcare's Definition Flash dualsource CT scanner. The impact of stent diameter on intra-lumen attenuation was evaluated using motion-free images, and the impact of heart rate on motion artifacts was evaluated using motion-containing images.

The findings demonstrated that attenuation deviations from normal rise with decreasing stent diameter, most likely as a function of the system's spatial resolution. Figure 7 shows that motion artifacts increased with heart rate and were greater for arteries that move the most, including the right coronary artery (RCA) and left circumflex (LCX), and less for the left coronary artery (LAD), which moves the least. Even at low heart rates, there were noticeable artifacts in the RCA. For better CT pictures at a lower patient dose, the pilot study demonstrated the significance of adjusting the time resolution with respect to heart rate and vessel location.

E. Compensation Methods for Voluntary Motion: PET Brain Imaging

In medical imaging, voluntary patient movements can also provide challenges, particularly for applications requiring lengthy acquisition times. The XCAT phantoms can be readily altered to mimic voluntary actions like shifting, repositioning, head movements, etc. because they are defined with NURBS surfaces. Rahmim et al.75 investigated a reconstruction-based compensation technique for PET brain imaging by simulating patient head motion using the XCAT. The XCAT was configured to replicate different head movements, and the PET image acquisition was simulated using Monte Carlo techniques. The data was reconstructed using a variety of techniques, including the one described in the article (Fig. 8). It is evident that the suggested approach significantly lowers motion artifacts both qualitatively and numerically.

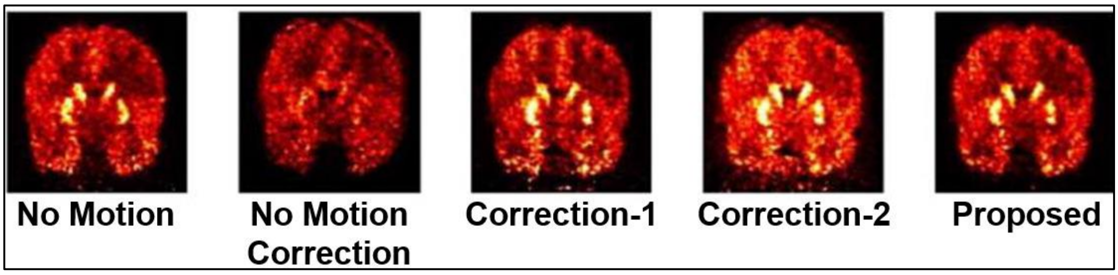

Fig. 8. PET simulations performed using an adult male XCAT phantom75 . Reconstructed images after 3 iterations (32 subsets); (column 1) no motion, (column 2) no motion correction, (column 3) Motion Correction Method 1, (column 4) Motion Correction Method 2, (column 5) a proposed Motion Correction reconstruction method. Coronal slices are shown.

Both the deliberate and involuntary movements of the patient are significant factors in biomedical imaging, according to earlier research. Designing procedures or techniques to lessen artifacts requires careful consideration. As shown in Table 1, numerous studies have been conducted to look into the impacts of motion and create compensatory techniques for them. Phantoms can be useful in this research because they can mimic motion.

3. RADIATION DOSIMETRY

Computerized phantoms offer a potent tool for studying radiation dosimetry in addition to refining system architecture, imaging technique, data gathering strategy, and image reconstruction and processing procedures. Concern over the potential population risk of ionizing radiation exposure is growing in medical imaging, especially with regard to nuclear medicine and x-ray CT76. Personalized medical procedures—that is, tailoring methods to each patient's characteristics (sex, age, body type) in order to provide diagnostic-quality images with the least amount of radiation—are a key field for future biomedical research and clinical use.

Computerized models, like the XCAT, offer a useful way to compare and optimize imaging applications in terms of radiation dose and image quality. It is possible to repeatedly simulate imaging of computational phantoms under a wide range of scanning parameters and situations without worrying about radiation exposure. As previously stated, it is feasible to compute the radiation exposure to the organs and tissues in addition to simulating medical images from computational phantoms. Monte Carlo techniques, which accurately model photon transit for various imaging procedures within a human or object as defined by a computational phantom, are commonly used for this.These techniques can be used to compute and compare the radiation exposure of the various organs, evaluate the impact of different scanning tools and parameters, and establish correlations that can be used to estimate patient doses.
Radiation dosimetry has greatly benefited from the employment of the XCAT phantom, Table 1. In order to precisely determine the radiation dosage from x-ray-based exams, we created and verified a Monte Carlo method77. The MC software can offer precise dosage estimates for certain individuals when paired with the XCAT models78. For comparison, the MC program can be used to model various imaging equipment and protocols79–81. Our library of XCAT models and our MC approach have been used in a number of research looking into dosimetry specific to patients and populations. The findings from a few representative studies are highlighted in the following.

A. Uncertainties in CT Dosimetry: XCAT as Compared to Other Computational Phantoms

For a representative set of CT protocols82, one study examined the uncertainty in CT dose and risk estimation related to various computational phantom types (in contrast to the XCAT models). This study's primary goal was to shed light on how various reference phantom types affect CT dosimetry in order to improve our understanding of the radiation dose that patients receiving CT exams experience.Thirteen standard body and neurological CT procedures had their organ dosages estimated. The LightSpeed VCT clinical system from GE Healthcare was simulated by the MC program77. Four approaches were employed for each protocol, each employing a distinct collection of reference phantoms: The standard adult male and female XCAT phantoms have organ masses that match those from ICRP 89 (values 83), as do the reference male and female phantoms described in ICRP publication 11084. Additionally, a commercial dosimetry spreadsheet (ImPACT group, London, England) has its own hermaphrodite stylized phantom (85), and another popular dosimetry spreadsheet (CT-Expo, Medizinische Hochschule, Hannover, Germany) has its associated male and female stylized phantoms (86).

Despite having nearly identical organ masses, total body weights, and heights, the analysis revealed that the phantoms' organ doses varied greatly because of differences in organ location, spatial distribution, and the dose approximation method (which was used to estimate dose to organs that were not explicitly defined because none of the phantoms had all radiosensitive organs). The findings highlight the significance of gathering a large number of precise, yet anatomically different, phantoms in order to capture the internal and exterior variances in patients, much like the findings of Section II.B.

B. Dose in CT and Other X-ray Based Modalities

Numerous thorough investigations have been conducted to look into the radiation dose and cancer risk for pediatric and adult CT87-90 patients. The Monte Carlo program77 was once more used to model common body and neurological CT protocols and the scan parameters that go along with them. The organ dose from several XCAT phantom subpopulations (adult and pediatric) was then estimated using the MC software. The data was used to assess the various aspects influencing dose, such as scanning parameters, patient age, and patient size.

As the average chest diameter of the phantom patient increased, it was discovered that the dose to the individual organs completely or partially inside the scan coverage decreased. The distance between the organ's center and the scan region's center was strongly correlated with the dose for the organs outside the scan coverage, although it was less correlated with patient size. This resulted from the fact that the absorption is exponentially proportional to the distance between the organ center outside the scan and the center of the scan region, but the dosage that was distributed to these organs was predominantly from dispersed radiation.

There was only a slight association between patient size and dosage to specific organs and the dose results from neurological procedures for the organs that were fully or partially within the scan coverage. Nonetheless, the correlation was often higher for the scattered organs (bone, marrow, and skin) and large organs (such the brain) that were fully contained within the appropriate scan coverage. Similar to the body protocols, the organ dose for the organs outside the scan coverage was highly connected with the separation between the organ's center and the scan region's center.

It was discovered that as patient size increased, the effective dose dropped significantly.

Table 2 Dose calculator developed based upon dose estimations from a series of XCAT adult phantoms90

Effective Dose (mSv)		
	MIN	MAX
ICRP 110	5.3	6.2
Organ Dose (mGy)		
Marrow	2.6	3
Bone	4.3	5.2
Skin	1.8	2.1
Brain	0.1	0,2
Eyes	0.1	0.1
Larynx-Pharynx	2.7	5.5
Thyroid	6.9	9.9
Esophagus	7.2	8.7
Lungs	9.1	10.1

Thymus	9.5	11.5
Breasts	7.4	10.1
Heart	9.3	10.7
Liver	5.3	7.3
Stomach	5.7	8

Body protocols showed a strong exponential correlation (r > 0.87), while neurological protocols showed a weaker correlation (r < 0.41), with the effective dose for neurological protocols more strongly correlated with the patient's measured trunk height than with the patient diameter. Normalized by the dose–length product (DLP), the organ and effective doses were found to be independent of collimation, pitch, and tube potential (<15% variation90), meaning that the results are largely scanner-independent and can be applied to other CT systems with reasonable accuracy. These figures are averaged across the entire population of phantoms or patients, but for a particular patient, the discrepancy can be as much as 25%89, 90.These findings suggest that we can generalize across scanners as a first order approximation. However, the precise scanner must be taken into consideration for accurate patient-specific organ dosage estimations.

In order to estimate the dose to patients, a dose estimation smartphone application90 was created based on the connections discovered in the investigations (Fig. 9). Radiologists can easily estimate and report a patient's dosage levels across a variety of CT scan procedures by using the dose calculator. The application is currently being expanded to encompass radiography and tomosyn thesis exams using methods akin to those described above. Our research led us to the conclusion that patient-specific dose estimates can be made using correlations between dose and patient size, age, and other variables (trunk length, organ center distance from scan center, etc.). These connections can offer direction for creating and refining imaging techniques,
modifying them to fit the unique needs of each patient. These correlations can be derived and their limitations can be identified using computational phantoms such as the XCAT.

C. Tube Current Modulation in CT

Many dose prediction methods, such as those above, are based on fixed tube current simulation while the majority of CT scans are being done with tube current modulation (TCM) techniques. Our simulation tools were used in a study to assess the effects of various TCM implementations on the organ dosage in the chest and abdomen-pelvis CT79.A female adult XCAT phantom was used as the patient in order to represent different TCM implementations in terms of modulation control strength, or α. The volume-weighted CT dose index (CTDIvol) was used to normalize organ dose in order to produce dose conversion factors that are mostly unaffected by scan parameters and system characteristics. It was discovered that the organ dose conversion factors strongly depended on α, indicating the necessity for organ dose conversion factors unique to TCM. A technique based on conversion factors developed for fixed-mA scans could be used to approximate organ dose for any α value (i.e., across modulation systems). This was accomplished by multiplying fixed-mA conversion factors by an organ CTDIvol that was obtained from the organ's location tube currents and the organ volume fluctuation along the longitudinal direction. According to the findings, organ conversion factors obtained from fixed-mA scans can be used to estimate organ doses for TCM scans with a good degree of accuracy (~20%) if one is aware of the mA modulation profiles. Therefore, utilizing simulated data from phantoms, a general method for evaluating organ dose across modulation methods for patients can be developed.

D. Effects of Contrast on CT Dosimetry

More than 60% of CT imaging studies include contrast enhancement. Contrast can alter the radiation dose by up to 70%91 in addition to having a significant effect on the quality of CT images. In order to replicate contrast dynamics92, a physiologically based pharmacokinetic (PBPK) model of the human circulatory system was recently created and integrated into the XCAT phantom framework. An first investigation on the effect of contrast media on radiation exposure in a standard CT abdominal scan93 was conducted using the improved XCAT models. In order to replicate patient-specific iodine concentration-time outcomes for a widely used uni-phasic IV injection technique, the dose estimation was carried out on 58 XCAT adult phantoms using the PBPK model.The dose as a function of time for a standard abdomen CT examination protocol utilized at our institution was estimated using MC techniques. The values computed for an unenhanced CT scan were contrasted with the time-varying organ and effective dose increment values. The contrast-based modeling findings showed that the normalized organ dosages increased by up to 53%. Compared to the unenhanced CT scan, the computed effective dosage normalized by DLP increased by up to 28%.The outcomes show how contrast enhancement may affect a patient's dosage. In a another investigation, the biological implications of this were examined for iodine contrast94. This study examined the link between radiation exposure and injected contrast material over time.

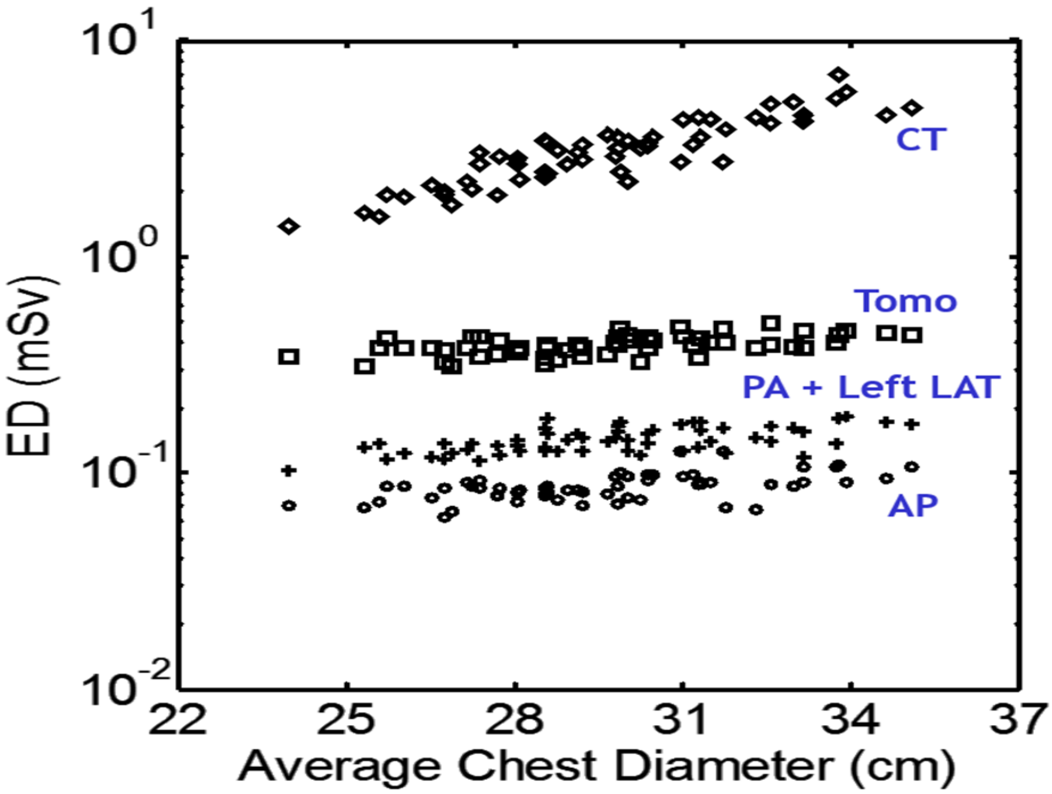

Fig. 10. Distribution of effective dose with respect to patient size for CT, Tomosynthesis (Tomo), posteroanterior + left lateral radiography (PA + Left LAT), and anteroposterior radiography (AP)95.

With increasing patient average chest diameter, the effective dose for CT increased considerably in an exponential fashion, while effective dose for radiographic modalities only increased slightly.
This can serve as a guide to help people provide contrast material as efficiently as possible in order to minimize dosage and any biological effects.

E. Comparison of Modalities

Comparing various imaging modalities is another use for dosimetry data from computerized phantoms. A clinical CT system (LightSpeed VCT, GE Healthcare) and a clinical radiography system (Definium 8000, VolumeRAD, GE Healthcare) utilized for chest radiography and tomosynthesis were contrasted in the Zhang et al.95 study.
Using standard procedures, the organ doses and effective doses were calculated from 59 adult male and female XCAT phantoms for each modality. Chest CT had the largest dosage, according to the simulated results, followed by radiography (1.3% that of chest CT) and tomosynthesis (12%), as shown in Fig. 10. Compared to radiography and tomosynthesis, it was discovered that the radiation dose from chest CT exams was significantly more influenced by the patient's body size.
This would suggest that larger patients might benefit more from chest tomosynthesis than CT.

F. Prospective Dosimetry

The XCAT phantoms can offer a radiation dose library from which to prospectively anticipate the radiation dosage for a specific patient before to the test, in addition to a patient base from which to research radiation dose retrospectively. In the subsequent study80, a specific XCAT phantom representing a chosen clinical patient was paired with another XCAT phantom in the library in an ideal manner (based on trunk height) to produce an anatomical representation of the patient. The two phantoms' organ doses were computed and compared using a clinical abdominal-pelvic CT technique. Each of the 58 adult XCAT models had this done.The anticipated organ dose (derived from the corresponding phantom) and the patient XCAT model's organ dose across all organs and modulation profiles agreed well in every phantom case. The outcomes of one matched pair of XCAT models are displayed in Figure 11.

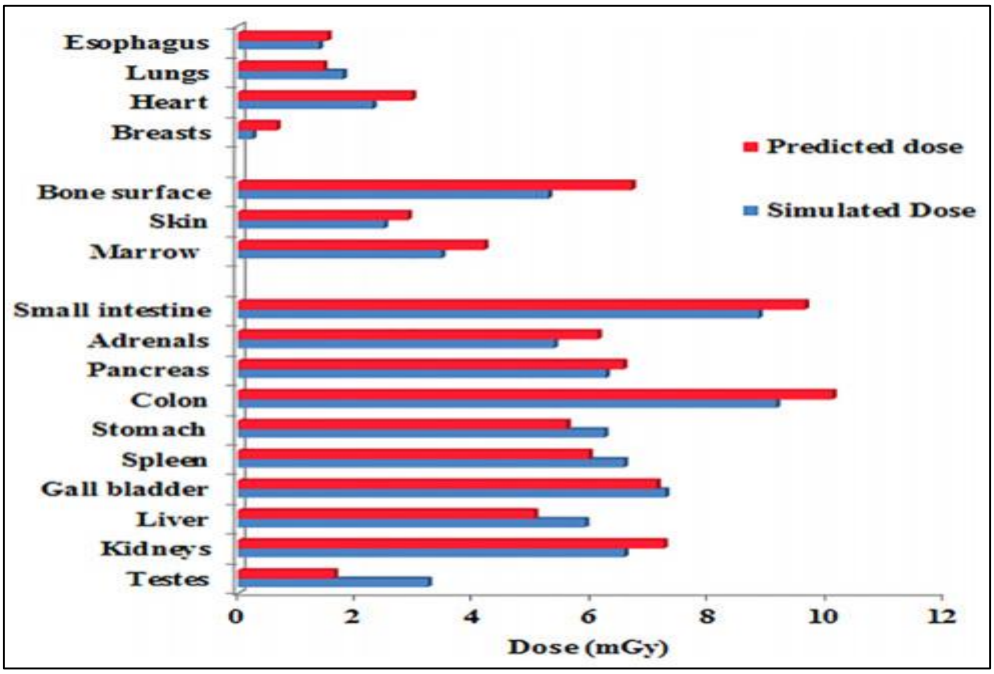

Fig. 11. Predicted and simulated organ dose for a patient undergoing a clinical abdominopelvic CT imaging protocol80 .

A new clinical patient can be matched to a matching model that closely resembles the patient in terms of the locations of key organs before their examination thanks to an atlas of computational phantoms that cover a wide range of human anatomy. Using MC approaches, dose measurements for the specific exam under different scanning conditions will have been pre-calculated. The dose that the patient will receive can be predicted using these measurements. With the knowledge of organ dose prior to a CT test, one can improve the CT protocol by modifying the scanning parameters to accomplish a goal diagnostic performance using such prediction models connected to picture quality measures.

4. RADIATION THERAPY

Radiation therapy (RT) has a significant challenge due to patient respiratory movements. In addition to differing from person to person, the motion also changes for various breaths within the same patient. New RT techniques need to be thoroughly validated, but a lot of patient data is needed to conduct an exhaustive evaluation and confirm the robustness of a particular methodology. Because of manufacturer-imposed limitations on clinical systems or radiation concerns, it might not be possible to get such data.Simulation methods and computational phantoms provide an alternate approach for radiation therapy research. The XCAT series of phantoms have been a useful tool for radiation therapy research because of its capacity to replicate various patient motions and anatomy, Table 1. Some applications in this field of study are shown in the section that follows.

A. 4D Radiotherapy Research Framework

To make it easier to characterize and use the XCAT models in 4D radiation treatment research96, an integrated Matlab application was created. It allows for the following functions: (1) creating 4D XCAT images using customized parameter files; (2) reviewing 4D XCAT images; (3) creating composite images from 4D XCAT images; (4) tracking motion of specific ROI regions; (5) converting XCAT raw binary images into a DICOM format; and (6) analyzing real-time position management (RPM) respiratory signals and clinically obtained 4D CT images.

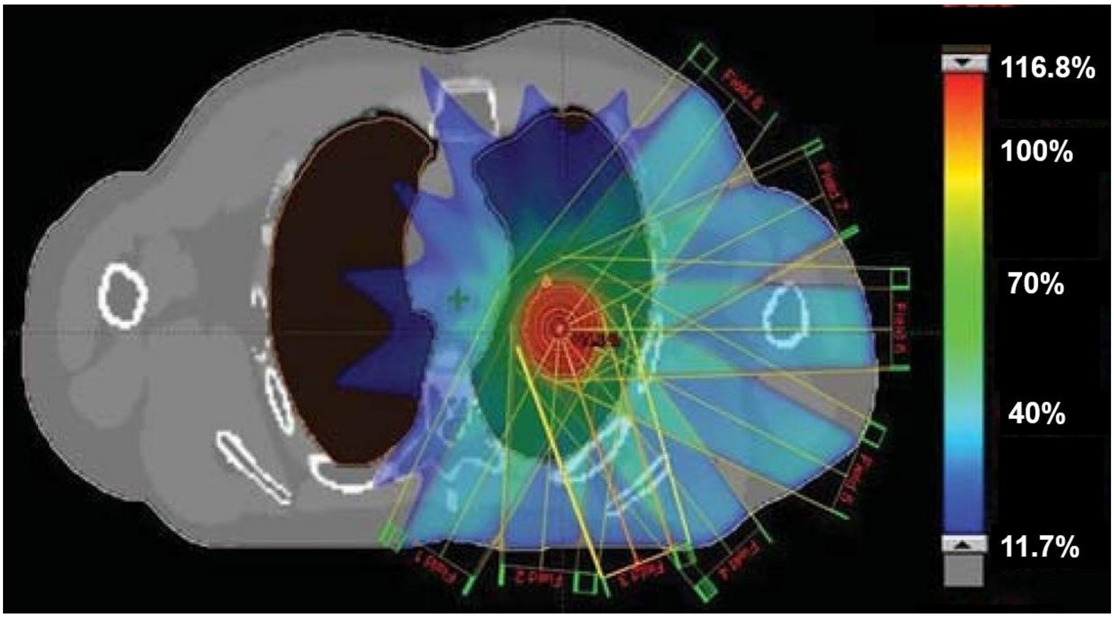

Fig. 12. Beam arrangement and dose distribution of a lung SBRT plan created on the XCAT phantom96. Colorbar shows Planning target volume dose (%).

The software allows the XCAT phantom's breathing pattern to be individually altered to replicate even intricate and erratic respiratory activity. Furthermore, the 4D XCAT phantom's anatomy can be altered to more closely resemble the anatomy of an actual patient. The 4D XCAT phantom's great degree of adaptability makes it a viable tool for patient-specific 4D quality control.For 4D RT research, the computer application created in this work can be utilized to create, examine, evaluate, process, and export 4D XCAT images. The beam configuration and dose distribution of the lung stereotactic body radiation therapy (SBRT) plan developed on a specific XCAT phantom are displayed in Figure 12. These outcomes are similar to actual patients' clinical goals. For 4D RT research, the application provides a strong workflow for implementing the 4D XCAT phantom. It is presently being used to research the best 4D CT imaging methods for RT.

C. Feasibility of 4D MRI

The clinical viability of a 4D MRI approach for radiation therapy97 has also been tested using the XCAT phantom as an alternative to CT. 4D MRI can improve soft-tissue contrast without appreciably increasing imaging time or expense, and it does not expose patients to radiation.

The suggested 4D-MRI method uses fast 2D cine-MR imaging to continually acquire axial images during the breathing cycle. The images are then retrospectively sorted by respiratory phase. The

breathing signal was extracted using the body region of the axial MR images as an internal respiratory surrogate. A male adult XCAT phantom was configured with the following settings in order to test the method:
maximum chest surface motion of 1.0 cm, maximum diaphragm motion of 3.0 cm, and a 5-second breathing duration. A liver spherical tumor with a diameter of 3 cm was modeled. The suggested technique's imaging procedure was then replicated by simulating 4D MRI images from the phantom while it was breathing properly. The simulated 4D MRI was used to calculate the tumor's motion trajectories, which were then compared to the known motions as produced by the 4D-XCAT. The tumor motion trajectory and the simulated images, Fig. 13, demonstrated a high degree of agreement with the known truth as supplied by the 4D-XCAT phantom. The outcomes showed that a new retrospective 4D-MRI method that use body area as a respiratory surrogate is feasible.Additional techniques for 4D MRI to enhance temporal/spatial resolution have been investigated using the XCAT phantom98, 99.

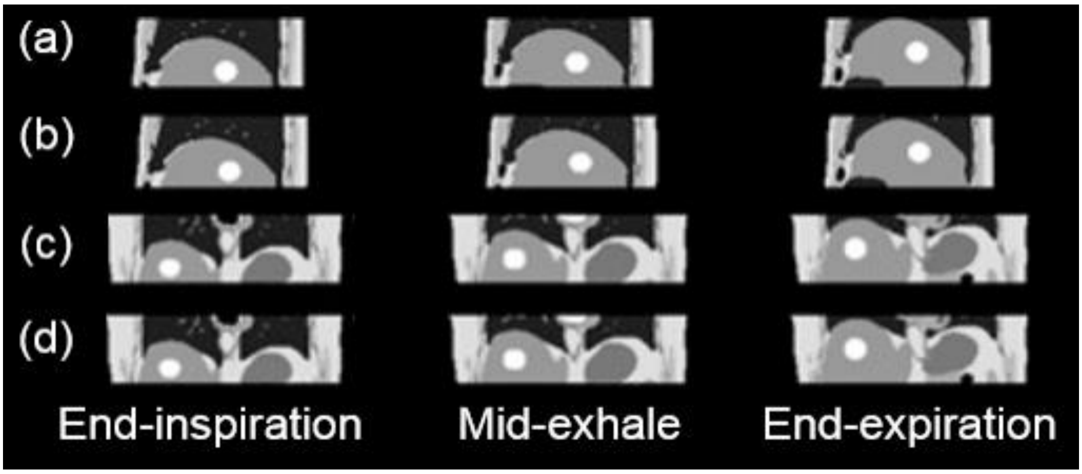

Fig. 13. Sagittal (a) and coronal (c) XCAT images compared to the sagittal (b) and coronal (d) images of simulated 4D-MRI97 .

C. 4D-Cone beam CT (CBCT) Development and Evaluation

The XCAT phantom is also being used to study 3D/4D cone-beam CT (CBCT) techniques. While 4D CBCT is a new on-board imaging technology for target localization, 3D CBCT is the method currently used for target localization before radiation delivery.
4D CT and 4D CBCT pictures are produced in different ways. 2D projections are obtained throughout several respiration cycles and then sorted by phase before reconstruction, as opposed to mixing reconstructed axial slices per respiratory phase. The acquired slice or projection must be linked with respiratory phase in order to produce 4D CBCT datasets; this is usually done by employing external markers as stand-ins for respiratory phase measurement. Nevertheless, it is unclear how these markers relate to respiratory motion, which may cause projections to not match.
Without the assistance of an external surrogate, a novel method based on the Fourier Transform theory was created to directly extract respiratory information from projections100. The XCAT phantoms101 was used in a simulation research to thoroughly assess the markerless approach.Different patient anatomy and variations in respiratory motion (such as shifts in the length of the respiratory cycle, the inspiration to expiration ratio, the amplitude of the diaphragm motion, the amplitude of the AP chest

wall motion, and the trajectories resulting from tumors and organs) were modeled using the phantoms. The study's findings showed how reliable the markerless method was across a range of anatomical and respiratory settings.

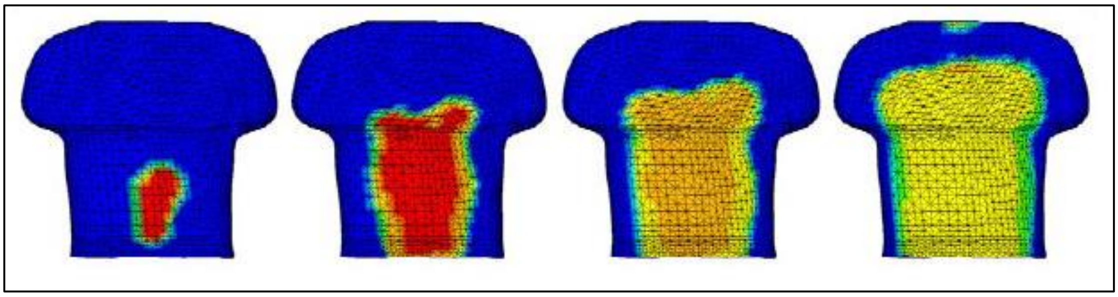

Fig. 14. Torso of an XCAT phantom showing the blast loading time progression, from left to right, for 0.10 ms, 0.12 ms, 0.140ms, and 0.18ms102 .

5. OTHER APPLICATIONS

The XCAT models have been used in research for the defense industry, electromagnetic (EM) radiation simulation, computational fluid dynamics (CFD), and medical device analysis and design, in addition to the aforementioned disciplines and outside of Table 1. The XCAT phantom is frequently transformed into a finite-element (FE) model for research in various fields.The Advanced Physics Laboratory (APL) at Johns Hopkins University102 conducted a study in which they manually transformed a 50th percentile male XCAT phantom's chest anatomy (weight and height) into a FE model. The FE model helped with the creation of personal protection equipment and was used to investigate the impact of blasts on the human torso.One computer simulation that depicts the blast pressure wave's evolution as it interacts with the XCAT's exterior is shown in Figure 14. The XCAT model in the aforementioned study underwent a time-consuming manual conversion into a FE model. A pipeline utilizing the ScanIP software was created in collaboration with Marc Horner from ANSYS and Kerim Genc from Simpleware to effectively transform the surface-based XCAT phantoms into FE models104 in order to conduct analysis for various applications.

Fig. 15. FE model of the XCAT arterial network103

In a study by Randles et al.103, ScanIP transformed the vasculature of a male adult XCAT phantom (50th percentile) into a FE model, which was subsequently utilized to explore quick computing techniques for simulating flow in arterial networks (Fig. 15). The concept is that the precise geometry of a patient's circulatory system can be determined using medical imaging. The computational cost of such models has hitherto limited the use of them in simulations. Patient-specific blood flow simulations for better diagnosis and treatment of patients with a variety of vascular disorders will be made possible by a quicker approach, like the one described here.

In a different study, Seckler et al.105 used a FE XCAT cardiac model to examine how several lead-depending and patient device factors affected the risk of electromagnetic interferences (EMIs) in patients with bipolar cardiovascular implantable electronic devices (CIEDs). Patients could be seriously at danger if EMIs cause CIEDs, such as pacemakers and implanted cardioverter-defibrillators, to malfunction.

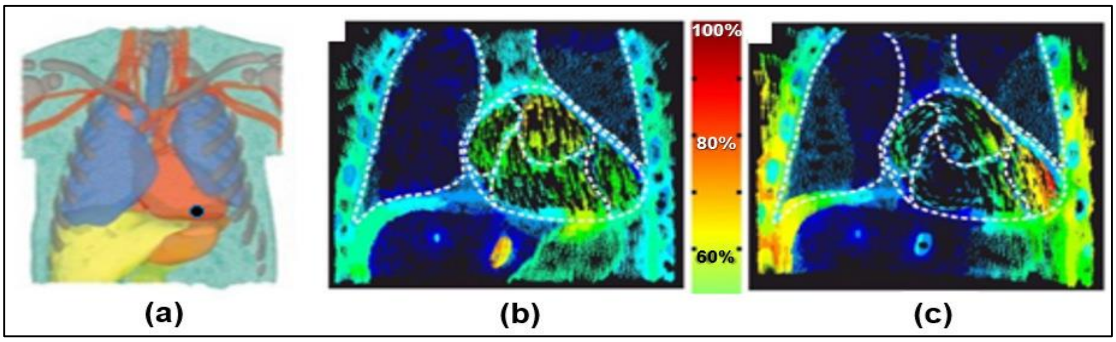

Fig. 16. FE cardiac simulations using the XCAT105. (a) The XCAT-male FE model, position of the tip electrode is indicated with a black dot. Current density distribution in the XCAT model for (b) the electric field and (c) the magnetic field. The color scale in the middle indicates the portion of the current density.

By computationally computing the voltage created in bipolar leads, the simulations utilizing the XCAT aimed to determine the risk of EMI for various CIED lead locations, heart positions in the thorax, and tissue conductivities of the organs. Example results for the current that is induced in the body by electric and magnetic fields are displayed in Figure 16. The current determines the voltage that is induced in the bipolar leads' distal end. The study showed that the position and orientation of the lead-tip are critical factors influencing the vulnerability of bipolar CIEDs through these simulations and comparison to human data.

6. CONCLUSIONS

The 4D XCAT phantoms, which were first created for biomedical imaging research, have found extensive application in a number of diverse sectors due to their capacity to accurately simulate human anatomy and physiology at all ages and body sizes. Some of those uses were mentioned in this review paper. The several XCAT tools and popular applications that have been used with it for study are compiled in Table 2 for your reference. There are other additional resources available as well, which can be obtained online and in literature.The various applications shown here demonstrate the growing significance of simulation tools and techniques in research. Researchers can conduct tests virtually through simulation that would not be feasible with live subjects otherwise. They are thus offering a useful alternative to clinical trials or perhaps a forerunner to them. It is frequently difficult or impossible to determine the actual illness state in clinical investigations. Second, obtaining a sufficient number of clinical studies is challenging, costly, time-consuming, and frequently extremely impractical or unattainable, even in cases where the truth is available. Some research might not even be ethically acceptable due to radiation issues.Although physical phantoms provide an alternative to live patients, creating a number of them that accurately reflect the different anatomical differences found in a community would be prohibitively costly. Furthermore, it is difficult to combine certain motions, such the heart and respiratory motions, into tangible test objects.Through the use of physics-based operators and user-defined computational phantoms, simulation offers a known reality that can be used to compare, optimize, and quantitatively assess various approaches. In a virtual environment, there are no restrictions; an infinite number of distinct anatomies or parameters can be created and examined. With the precise controls provided in the virtual domain, simulation enables researchers to answer basic issues that can only be practically solved through rapid and economical experimentation.Virtual approaches could even take the place of genuine clinical trials if they are realistic enough. More realism is the goal of current computer phantom development study. Like other computational models, the XCAT phantom still has a lot of potential to develop despite its advancements and usefulness. The uses of the XCAT in medical imaging serve as one example of this. The phantom has mostly been utilized for lower resolution modalities like nuclear medicine, aside from dosimetry. The organs and structures in the XCAT phantoms are homogeneous, similar to contemporary computational phantoms, and only contain simplified, geometrical models for diseases.

Table 3. Summary of tools developed for the XCAT and common programs used with it. Different phantom representations (voxelized, FE mesh, polygon mesh, or NURBS surfaces) are required for different programs. XCAT tools indicated by an asterisk can be obtained by contacting paul.

***XCAT phantom software and models**
XCAT program: generates phantoms (typically within minutes) as voxelized images, NURBS or polygon mesh surfaces given user-defined parameters XCAT library of phantoms: work with the XCAT program or can be saved in a variety of 3D formats (stl, iges, obj, step, sat, dxf, etc.)
Tools to view XCAT phantoms as voxelized images
ImageJ, imagej.nih.gov/ij AMIDE, amide.sourceforge.net ANALYZE, analyzedirect.com MATLAB, www.mathworks.com/products/matlab.html Any program that can read raw binary images (32 bit float, little endian)
Tools to view XCAT phantoms as surfaces
Rhinoceros, www.rhino3d.com *Rhinoscripts to input/output the phantoms
Tools to deform or reposition the XCAT phantoms
Anatomical and motion parameters within the XCAT software8 *Rhinoscripts to manipulate XCAT surfaces within Rhinoceros software
Tool to convert XCAT phantoms into FE models to input into FE analysis software
ScanIP, www.simpleware.com/software/scanip/
Monte Carlo methods for simulating SPECT, PET, and X-ray projection data and calculating radiation dose from XCAT phantoms (operate mostly on voxelized representations of the phantoms, some may include the ability to use NURBS or polygon meshes)
MCNP, mcnp.lanl.gov SIMIND, www.msf.lu.se/forskning/the-simind-monte-carlo-program SimSET, depts.washington.edu/simset/html/simset_main.html EGSnrc, www.nrc-cnrc.gc.ca/eng/solutions/advisory/egsnrc_index.html GATE, www.opengatecollaboration.org/ GEANT-4, geant4.cern.ch/ PENELOPE, www.oecd-nea.org/tools/abstract/detail/nea-1525 Li et al.77
***Analytical method for simulating X-ray projection data from XCAT phantoms (calculates projections directly from the NURBS surface definition of the phantoms without voxelization)**
XCAT X-ray projector106
Reconstruction algorithms for reconstructing SPECT, PET, or X-ray projection data into medical images
Users typically use their own software Reconstruction packages such as the Michigan Image Reconstruction Toolbox

(MIRT), web.eecs.umich.edu/~fessler/code, are also publically available
MRI simulators for generating MRI images from XCAT phantoms
MRISIM107, github.com/BIC-MNI/mrisim OD1N, http://od1n.sourceforge.net/

Because of this, the phantoms are limited in their ability to evaluate picture quality in higher resolution modalities like CT and MRI, even if they are sufficient for dosimetry experiments. Fig. 6 illustrates how wildly unrealistic the visuals created by them are. We are also looking at using volumetric textures109 to describe the inner variability of the structures in the XCAT phantoms and adding finer anatomical detail for extra structure definition108 in order to get around this restriction.The usage of XCAT phantoms and other computational models in biomedical and bioengineering research will only increase as they become more realistic. The utilization and value of the XCAT phantoms in virtual simulations are anticipated to grow with the development of newer techniques and applications, such as dynamic perfusion and textured organs.

REFERENCES

1. Xu XG. An exponential growth of computational phantom research in radiation protection, imaging, and radiotherapy: a review of the fifty-year history. Phys Med Biol. 2014;59:R233-302

2. Gosselin MC, Neufeld E, Moser H, Huber E, Farcito S, Gerber L, et al. Development of a new generation of high-resolution anatomical models for medical device evaluation: the Virtual Population 3.0. Phys Med Biol. 2014;59:5287-5303 Zygote Anatomy Collection, https://www.zygote.com/.

4. TurboSquid 3D Models, https://www.turbosquid.com.

5. Free3D, https://free3d.com/3d-models/human.

6. Global Human Body Models Consortium, http://www.ghbmc.com/.

7. Human Body Models, http://www.humanbodymodels.com/.

8. Segars WP, Mendonca S, Grimes J, Sturgeon G, Tsui BMW. 4D XCAT phantom for multimodality imaging research. Medical Physics. 2010;37:4902-4915

9. Segars WP. Development of a new dynamic NURBS-based cardiac-torso (NCAT) phantom., PhD dissertation,. May 2001;Ph.D.

10. Segars WP, Lalush DS, Tsui BMW. A realistic spline-based dynamic heart phantom. IEEE Transactions on Nuclear Science. 1999;46:503-506

11. Segars WP, Lalush DS, Tsui BMW. Modeling respiratory mechanics in the MCAT and spline-based MCAT phantoms. IEEE Trans. Nucl. Sci. 2001;48:89-97

12. Axelsson B, Persliden J, Schuwert P. Dosimetry for computed tomography examination of children. Radiat Prot Dosim. 1996;64:221-226

13. Segars WP, Bond J, Frush J, Hon S, Eckersley C, Williams CH, et al. Population of anatomically variable 4D XCAT adult phantoms for imaging research and optimization. Med Phys. 2013;40:043701

14. Norris H, Zhang Y, Bond J, Sturgeon GM, Minhas A, Tward DJ, et al. A set of 4D pediatric XCAT reference phantoms for multimodality research. Med Phys. 2014;41:033701

15. Segars W, Norris H, Sturgeon G, Zhang Y, Bond J, Minhas A, et al. The development of a population of 4D pediatric XCAT phantoms for imaging research and optimization. Medical Physics. 2015;42

16. Heimann T, Meinzer H-P. Statistical shape models for 3D medical image segmentation: A review. Medical Image Analysis. 2009;13:543-563
17. Zeng D, Gong C, Bian Z, Huang J, Zhang X, Zhang H, et al. Robust dynamic myocardial perfusion CT deconvolution for accurate residue function estimation via adaptive-weighted tensor total variation regularization: a preclinical study. Phys Med Biol. 2016;61:8135-8156
18. Kim JH, Chang Y, Ra JB. Denoising of polychromatic CT images based on their own noise properties. Med Phys. 2016;43:2251
19. Slavine NV, Guild J, McColl RW, Anderson JA, Oz OK, Lenkinski RE. An iterative deconvolution algorithm for image recovery in clinical CT: A phantom study. Phys Med. 2015;31:903-911
20. Gong C, Zeng D, Bian Z, Zhang H, Zhang Z, Zhang J, et al. [Robust low-dose CT myocardial perfusion deconvolution via high-dimension total variation regularization]. Nan Fang Yi Ke Da Xue Xue Bao. 2015;35:1579-1585
21. Cooper BJ, O'Brien RT, Kipritidis J, Shieh CC, Keall PJ. Quantifying the image quality and dose reduction of respiratory triggered 4D cone-beam computed tomography with patientmeasured breathing. Phys Med Biol. 2015;60:9493-9513
22. Zhang Y, Ma J, Iyengar P, Zhong Y, Wang J. A new CT reconstruction technique using adaptive deformation recovery and intensity correction (ADRIC). Med Phys. 2017
23. Gong C, Han C, Gan G, Deng Z, Zhou Y, Yi J, et al. Low-dose dynamic myocardial perfusion CT image reconstruction using precontrast normal-dose CT scan induced structure tensor total variation regularization. Phys Med Biol. 2017;62:2612-2635
24. Zhong Z, Gu X, Mao W, Wang J. 4D cone-beam CT reconstruction using multi-organ meshes for sliding motion modeling. Phys Med Biol. 2016;61:996-1020
25. Zeng D, Gao Y, Huang J, Bian Z, Zhang H, Lu L, et al. Penalized weighted least-squares approach for multienergy computed tomography image reconstruction via structure tensor total variation regularization. Comput Med Imaging Graph. 2016;53:19- 29
26. Rigie DS, La Riviere PJ. Joint reconstruction of multi-channel, spectral CT data via constrained total nuclear variation minimization. Phys Med Biol. 2015;60:1741-1762
27. Mihlin A, Levin C. An Expectation Maximization Method for Joint Estimation of Emission Activity Distribution and Photon Attenuation Map in PET. IEEE Trans Med Imaging. 2016
28. Ashrafinia S, Mohy-Ud-Din H, Karakatsanis NA, Jha AK, Casey ME, Kadrmas DJ, et al. Generalized PSF modeling for optimized quantitation in PET imaging. Phys Med Biol. 2017;62:5149-5179
29. Gianoli C, Riboldi M, Fontana G, Kurz C, Parodi K, Baroni G. A sinogram warping strategy for pre-reconstruction 4D PET optimization. Med Biol Eng Comput. 2016;54:535-546
30. Chan C, Dey J, Grobshtein Y, Wu J, Liu YH, Lampert R, et al. The impact of system matrix dimension on small FOV SPECT reconstruction with truncated projections. Med Phys. 2016;43:213
31. Vieira L, Costa DC, Almeida P. The influence of number of counts in the myocardium in the determination of reproducible functional parameters in gated-SPECT studies simulated with GATE. Rev Esp Med Nucl Imagen Mol. 2015;34:339-344
32. Zhang X, Zhou J, Cherry SR, Badawi RD, Qi J. Quantitative image reconstruction for total-body PET imaging using the 2-meter long EXPLORER scanner. Phys Med Biol. 2017;62:2465-2485
33. Karakatsanis NA, Tsoumpas C, Zaidi H. Quantitative PET image reconstruction employing nested expectation-maximization deconvolution for motion compensation. Comput Med Imaging Graph. 2016

34. Ihsani A, Farncombe TH. A Kernel Density Estimator-Based Maximum A Posteriori Image Reconstruction Method for Dynamic Emission Tomography Imaging. IEEE Trans Image Process. 2016;25:2233-2248
35. Abdalah M, Boutchko R, Mitra D, Gullberg GT. Reconstruction of 4-D dynamic SPECT images from inconsistent projections using a Spline initialized FADS algorithm (SIFADS). IEEE Trans Med Imaging. 2015;34:216-228
36. Su KH, Yen TC, Fang YH. A novel approach for direct reconstruction of parametric images for myocardial blood flow from PET imaging. Med Phys. 2013;40:102505
37. Zhang D, Yang BH, Wu NY, Mok GS. Respiratory average CT for attenuation correction in myocardial perfusion SPECT/CT. Ann Nucl Med. 2017;31:172-180
38. Mok GS, Sun T, Huang TC, Vai MI. Interpolated average CT for attenuation correction in PET--a simulation study. IEEE Trans Biomed Eng. 2013;60:1927-1934
39. Noori-Asl M, Sadremomtaz A, Bitarafan-Rajabi A. Evaluation of three scatter correction methods based on estimation of photopeak scatter spectrum in SPECT imaging: a simulation study. Phys Med. 2014;30:947-953
40. Song N, Du Y, He B, Frey EC. Development and evaluation of a model-based downscatter compensation method for quantitative I- 131 SPECT. Med Phys. 2011;38:3193-3204
41. Khoshakhlagh M, Pirayesh Islamian J, Abedi SM, Mahmoudian B, Shayesteh Azar M. A Monte Carlo study for optimizing the detector of SPECT imaging using a XCAT human phantom. Nucl Med Rev Cent East Eur. 2017;20:10-14
42. Ghaly M, Du Y, Links JM, Frey EC. Collimator optimization in myocardial perfusion SPECT using the ideal observer and realistic background variability for lesion detection and joint detection and localization tasks. Phys Med Biol. 2016;61:2048-2066
43. Chun SY, Fessler JA, Dewaraja YK. Correction for collimatordetector response in SPECT using point spread function template. IEEE Trans Med Imaging. 2013;32:295-305
44. Mao Y, Yu Z, Zeng GL. Segmented slant hole collimator for stationary cardiac SPECT: Monte Carlo simulations. Med Phys. 2015;42:5426-5434
45. Islamian JP, Toossi MT, Momennezhad M, Zakavi SR, Sadeghi R, Ljungberg M. Monte carlo study of the effect of collimator thickness on T-99m source response in single photon emission computed tomography. World J Nucl Med. 2012;11:70-74